This is a repository copy of *Stomatal dynamics in Alloteropsis semialata arise from the evolving interplay between photosynthetic physiology, stomatal size and biochemistry*.

White Rose Research Online URL for this paper:
https://eprints.whiterose.ac.uk/215420/

Version: Published Version

Article:
Zhou, Y. orcid.org/0000-0002-1837-9261 and Osborne, C.P. orcid.org/0000-0002-7423-3718 (2024) Stomatal dynamics in Alloteropsis semialata arise from the evolving interplay between photosynthetic physiology, stomatal size and biochemistry. Plant, Cell & Environment, 47 (12). pp. 4586-4598. ISSN 0140-7791

https://doi.org/10.1111/pce.15047

Reuse
This article is distributed under the terms of the Creative Commons Attribution (CC BY) licence. This licence allows you to distribute, remix, tweak, and build upon the work, even commercially, as long as you credit the authors for the original work. More information and the full terms of the licence here: https://creativecommons.org/licenses/

Takedown
If you consider content in White Rose Research Online to be in breach of UK law, please notify us by emailing eprints@whiterose.ac.uk including the URL of the record and the reason for the withdrawal request.

eprints@whiterose.ac.uk
https://eprints.whiterose.ac.uk/

Check for updates

Received: 29 September 2023 | Accepted: 8 July 2024

DOI: 10.1111/pce.15047

ORIGINAL ARTICLE

Plant, Cell & Environment | WILEY

Stomatal dynamics in *Alloteropsis semialata* arise from the evolving interplay between photosynthetic physiology, stomatal size and biochemistry

Yanmin Zhou | Colin P. Osborne

Plants, Photosynthesis and Soil, School of Biosciences, University of Sheffield, Sheffield, UK

Correspondence
Colin P. Osborne, Plants, Photosynthesis and Soil, School of Biosciences, University of Sheffield, Sheffield, UK.
Email: c.p.osborne@sheffield.ac.uk

Funding information
China Scholarship Council

Abstract

C_4 plants are expected to have faster stomatal movements than C_3 species because they tend to have smaller guard cells. However, little is known about how the evolution of C_4 photosynthesis influences stomatal dynamics in relation to guard cell size and environmental factors. We studied photosynthetically diverse populations of the grass *Alloteropsis semialata*, showing that the origin of C_4 photosynthesis in this species was associated with a shortening of stomatal guard and subsidiary cells. However, for a given cell size, C_4 and C_3–C_4 intermediate individuals had similar or slower light-induced stomatal opening speeds than C_3 individuals. Conversely, when exposed to decreasing light, stomata in C_4 plants closed as fast as those in non-C_4 plants. Polyploid formation in some C_4 plants led to larger stomatal cells and was associated with slower stomatal opening. Conversely, diversification of C_4 diploid plants into wetter environments was associated with an acceleration of stomatal opening. Overall, there was significant relationship between light-saturated photosynthesis and stomatal opening speed in the C_4 plants, implying that photosynthetic energy production was limiting for stomatal opening. Stomatal dynamics in this wild grass therefore arise from the evolving interplay between photosynthetic physiology and the size and biochemical function of stomatal complexes.

KEYWORDS
C_3 photosynthesis, C_4 photosynthesis, climate, evolution, stomatal dynamics

1 | INTRODUCTION

Gas exchange is fundamental for plant growth and yield, such that carbon gain comes at the cost of significant water loss (Brestic et al., 2018; Matthews et al., 2017). Enhancing photosynthesis while reducing water loss has therefore become an important target for crop improvement (Lawson & Blatt, 2014; Long et al., 2006). Several strategies are being applied to enhance carbon fixation, for example: the optimisation of photosynthetic enzymes (e.g., Rubisco, ATP synthase and phosphoribulokinase) and the Calvin–Benson–Bassham cycle, introducing the C_4 and non-plant carbon concentrating mechanisms into C_3 plants, improving mesophyll conductance to CO_2 and optimising responses to fluctuating light conditions (Kaiser et al., 2019; Orr et al., 2017). However, the balance between carbon gain and water loss largely depends on stomatal

This is an open access article under the terms of the Creative Commons Attribution License, which permits use, distribution and reproduction in any medium, provided the original work is properly cited.
© 2024 The Author(s). *Plant, Cell & Environment* published by John Wiley & Sons Ltd.

behaviour, and this has been less well studied than carbon fixation. Therefore, to increase leaf water-use efficiency (WUE), more attention is now being paid to the physiological responses of stomatal conductance (g_s) to environmental conditions (Matthews et al., 2020; Ozeki et al., 2022; Vialet-Chabrand et al., 2017).

Stomatal aperture is regulated via internal signals in response to environmental cues (light, CO_2), to ensure that leaves balance gaseous diffusion (Lawson & Blatt, 2014). The speeds of stomatal opening and closing depend on several factors, including direct effects like stomatal size and morphology (Faralli et al., 2019; Lawson & Blatt, 2014), and indirect influences such as plant water status (Durand et al., 2020; Ozeki et al., 2022) and photosynthetic pathway (McAusland et al., 2016; Ozeki et al., 2022). Many previous studies have shown that both the size and density of stomata are important, since they combine to influence the rate of stomatal movements and set the maximum value of g_s (Faralli et al., 2019; Lawson & Blatt, 2014; Vialet-Chabrand et al., 2017). In particular, smaller guard cells have a high surface-area-to-volume ratio, causing them to change osmotic pressure via the active transport of ions across the cell membrane more rapidly than larger cells. They also have smaller pores to shut and less distance to move. In combination, these factors enable them to close faster than larger guard cells in response to changing environmental cues (Faralli et al., 2019; Raven, 2014).

Previous work has shown that C_4 plants in general have evolved smaller stomata for a given stomatal density (SD; Table S1) than C_3 plants, leading to a lower maximum value for g_s (Taylor et al., 2012). This adaptation arises because C_4 photosynthesis increases the CO_2 concentration around the CO_2-fixing enzyme Rubisco (Bräutigam & Gowik, 2016), which enables C_4 plants to maintain carbon fixation at a lower diffusive conductance (and therefore a higher WUE) than C_3 plants. Smaller stomata at a higher density in C_4 crops are associated with rapid stomatal movements (McAusland et al., 2016), which are faster than those in C_3 species (Ozeki et al., 2022). However, under high nitrogen conditions the difference is explained by stomatal size and density, such that stomatal speed follows a common relationship with stomatal size or density in C_4 and C_3 crops (Ozeki et al., 2022). The effect of photosynthetic pathway acts in addition to the rapid environmental responses of dumbbell-shaped guard cells typical of grasses and some other monocots (McAusland et al., 2016). Both the size and shape of guard cells may therefore influence the range of possible speeds in C_4 and C_3 species.

We have used the grass *Alloteropsis semialata* as a model for investigating the evolution of photosynthetic physiology in C_3 and C_4 plants, since it shows a high level of intraspecific variation in photosynthesis, including intermediate forms (Lundgren et al., 2016). As a grass (Poaceae), its guard cells are of the dumbbell-shaped type, and guard cell size varies in relation to polyploidy (Linder et al., 2018). These features make *A. semialata* a good study system for investigating how stomatal function changes with photosynthetic pathway and guard cell size. Its large geographical distribution across Africa, Asia and Oceania offers the additional opportunity to investigate whether stomatal function adapts to local climatic conditions. In this paper, we use populations of *A. semialata* sampled from across its geographical range (Figure 1; Table S2) to investigate how natural variation in photosynthetic type, cell size and habitat conditions influence dynamic stomatal responses to changing light conditions. We test the hypotheses that: (i) C_4 pathway evolution gives rise to smaller guard cells in C_4 diploid populations, which have faster stomatal responses to light than in the C_3 type because of their smaller size; (ii) the larger guard cells of polyploids are slower responding than the smaller guard cells of diploids; and (iii) warm and dry environmental conditions select for stomata with a water-conserving strategy of slow opening and fast closure.

2 | MATERIALS AND METHODS

2.1 | Plant material and bioclimatic variables

Plants of *A. semialata* with various photosynthetic types (C_3, C_3–C_4 and C_4) and ploidy levels (diploid, hexaploid and dodecaploid) from 18

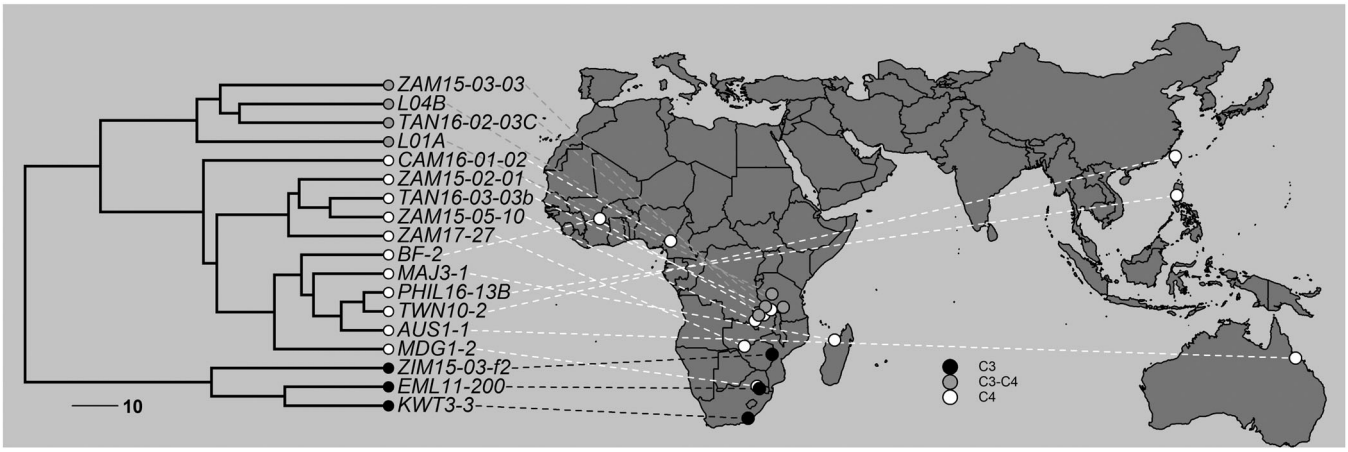

FIGURE 1 Phylogeny and geographical distribution of the sampled populations in *Alloteropsis semialata*. The phylogeny depicts evolutionary relationships between C_3 (black, $n = 3$ populations), C_3–C_4 intermediates (grey, $n = 4$ populations) and C_4 (white, $n = 11$ populations).

13653040, 0, Downloaded from https://onlinelibrary.wiley.com/doi/10.1111/pce.15047 by University Of Sheffield, Wiley Online Library on [01/08/2024]. See the Terms and Conditions (https://onlinelibrary.wiley.com/terms-and-conditions) on Wiley Online Library for rules of use; OA articles are governed by the applicable Creative Commons License

geographic origins (Figure 1; Table S2) were collected in this study (Bianconi et al., 2020; Lundgren et al., 2016). There were 11 populations with three replicates, four populations with two replicates, two populations with one plant, and one population with five replicates, according to the collection of plants. A total 48 individuals were involved in this study. Plants were grown in plastic pots (sized 1 L) containing John Innes No. 2 compost (John Innes Manufacturers Association) and fertilised once a month with Scotts Evergreen Lawn Food (The Scotts Company). Experiments were carried out in 2021.

The values of bioclimatic variables including annual precipitation were extracted from the WorldClim database (Alenazi et al., 2023; Fick & Hijmans, 2017) based on the geographic coordinates of collection locations of populations, using the Raster package (Alenazi et al., 2023; Hijmans, 2023) in R software (http://www.r-project.org/, version 4.2.1).

2.2 | Phylogeny and genome sizes

For molecular dating, 100 sets of five randomly chosen Benchmarking Universal Single-Copy Orthologs (BUSCO) genes were selected and analysed to produce a set of trees that represented the various histories existing within the genomes. A reference-based method (Dunning, Moreno-Villena, et al., 2019; Olofsson et al., 2016, 2019), with the chromosome-scale genome of an Australian individual of *A. semialata* (AUS1-1; Dunning, Olofsson, et al., 2019) as a reference was used to generate consensus sequences for each BUSCO. Full details of molecular dating are provided in Raimondeau et al. (2023). A time-calibrated phylogenetic tree for *A. semialata* was generated based on nuclear genomes under a coalescence model by Bayesian inference as implemented in *Beast2 v.2.6.4 (Bouckaert et al., 2019; Raimondeau et al., 2023). The DNA substitution model was set to a GTR + G as its reliable across most genes (Abadi et al., 2019), and the relaxed molecular clock with a log-normal distribution of rates was applied. Each individual was set as a different species to obtain a phylogenetic tree that indicates the relationships among accessions. The specific approach of generating a summary tree and mapping the median ages on nodes of the highest credibility tree is provided in Bouckaert (2010) and Raimondeau et al. (2023).

Genome sizes of some *A. semialata* individuals were estimated using the Sysmex Partec Cyflow SL3 flow cytometry, following the method with minor modifications described by Doležel et al. (2007) and Bianconi et al. (2020). Ebihara with 3% PVP was applied to the fresh samples, which were analysed by a flow cytometer fitted with a 100 mW green solid-state laser (Cobalt Samba). According to the internal calibration standards, for diploid populations, *Petroselinum crispum* 'Champion Moss Curled' (4.5 pg/2 C) was used, while for populations with C-values more than three times larger than any diploids, *Pisum sativum* 'Ctirad' (9.09 pg/2 C) was used (Bianconi et al., 2020). Data for the remaining *A. semialata* individuals were retrieved from previous publications (Bianconi et al., 2020; Olofsson et al., 2016, 2021). Ploidy levels were assigned based on the estimates of genome size for individuals with known chromosome numbers and genome size (Bianconi et al., 2020).

2.3 | Stomatal traits

Stomatal impressions were taken from two surfaces of the same leaves measured in gas exchange experiments. Dental putty (President Plus-light body; Coltène/Whaledent Ltd.) impressions were produced following the methods of Weyers and Johansen (1985) and Dunn et al. (2019), and nail polish peels made from impressions were transferred onto microscope slides. Guard cell length (GCL), guard cell width (GCW), subsidiary cell length (SCL), subsidiary cell width (SCW) and SD were measured using Image Pro-Plus 6.0 (Media Cybernetics). Guard cell surface area (GCSA) and guard cell volume (GCV) were estimated by assuming that guard cells are shaped like capsules, that is, cylindrical with hemispherical ends (Raven, 2014). Full details are provided by Raven (2014). GCSA to volume ratio (GCSA:GCV) was calculated as GCSV/GCV.

Maximum stomatal conductance to water vapour (g_{max}) as limited by anatomical constraints was calculated as the sum of abaxial and adaxial maximum conductance values for each leaf. Values of g_{max} on each leaf surface were estimated using the equations of Weyers and Meidner (1990) and Franks and Farquhar (2001):

$$g_{max} = d \times SD \times a_{max} / \left(v \times \left(l + \left(\frac{\pi}{2} \right) \times \sqrt{\frac{a_{max}}{\pi}} \right) \right), \quad (1)$$

where d is the diffusivity of water in the air at 22°C ($m^2\ s^{-1}$), SD is stomatal density (mm^{-2}), a_{max} is the mean maximum stomatal pore area (μm^2), v is the molar volume of air at 22°C ($m^3\ mol^{-1}$), l is pore depth (μm) that is equal to the GCW, π is the mathematical constant (~3.142) and l is assumed to be equivalent to GCW (μm) in the middle of the stoma (McAusland et al., 2016; Taylor et al., 2012).

2.4 | Leaf gas exchange

All photosynthetic parameters were measured using the LI-COR 6400XT portable gas-exchange system with a 6400-40 fluorometer head unit (LI-COR). Gas exchange measurements were carried out on the youngest fully expanded leaf of well-watered plants. The LI-COR cuvette conditions during gas exchange measurements were controlled as follows: a CO_2 concentration of 400 μmol mol^{-1}, a leaf temperature of 24 ± 1°C, a leaf vapour pressure deficit in the range 1.4–1.9 kPa, and a flow rate of 500 μmol s^{-1}.

The responses of net CO_2 assimilation (A) and stomatal conductance (g_s) to a step-change in photosynthetic photon flux density (PPFD) were carried out as described using the method of McAusland et al. (2016), with the following changes to the protocol: (i) leaves were equilibrated to a PPFD of 100 μmol $m^{-2}\ s^{-1}$ until both A and g_s were at a steady state; (ii) *PPFD* was then increased to 1000 μmol $m^{-2}\ s^{-1}$ for 1 h until a new steady-state was reached with A and g_s recorded every 30 s, before returning to 100 μmol $m^{-2}\ s^{-1}$ for a further 1 h to reach the final steady state.

13653040, 0, Downloaded from https://onlinelibrary.wiley.com/doi/10.1111/pce.15047 by University Of Sheffield, Wiley Online Library on [01/08/2024]. See the Terms and Conditions (https://onlinelibrary.wiley.com/terms-and-conditions) on Wiley Online Library for rules of use; OA articles are governed by the applicable Creative Commons License

The same leaf was used during the same day to record the relationship between steady-state g_s and irradiance. Measurements were recorded every 30 s starting from low irradiance to high irradiance levels (0, 50, 100, 200, 400, 800, 1200, 1600, 2000 μmol m^{-2} s^{-1}). Each irradiance level was provided for at least 30 min to reach a steady-state value of g_s (Ng & Jarvis, 1980).

2.5 | Modelling stomatal responses to a fluctuating environment

Stomatal dynamics to irradiance were fitted to an empirical descriptive sigmoidal model (Figure S1) according to Vialet-Chabrand et al. (2013) and McAusland et al. (2016), such that:

$$g_t = g_0 + (G_s - g_0) \times e^{-e^{(\lambda - t)/k + 1)}}, \quad (2)$$

where g_t is the stomatal conductance at time t. $g_0 = g_t$, when $t = 0$. Gs is the steady-state g_s for a given PPFD, and λ is the initial lag time. To distinguish between time delays for stomatal opening (increase) or closure (decrease), the abbreviations λ_i and λ_d were used. The parameter k is a response time constant. As with λ_i and λ_d, k_i and k_d were used to indicate the time taken for the stomata to open and close.

The maximum slopes of g_s responses (SI_{max}) to a change in PPFD was calculated as:

$$SI_{max} = \frac{G_s - g_0}{k \times e}. \quad (3)$$

The steady-state value of A_s was described as a function of PPFD using a non-rectangular hyperbola function:

$$A_s = \frac{\alpha_i PPFD + (A_{sat} + R_d) - \sqrt{(\alpha_i PPFD + (A_{sat} + R_d))^2 - 4\theta\alpha_i PPFD(A_{sat} + R_d)}}{2\theta} - R_d, \quad (4)$$

where α_i is the quantum yield of photosynthesis on an incident light basis, θ is the curvature parameter, A_{sat} is the light-saturated CO_2 assimilation rate and R_d is the rate of dark respiration. The steady-state parameter A_{sat} was estimated from this curve.

2.6 | Statistical analysis

R software (http://www.r-project.org/, version 4.2.1) was used to statistically analyse the data and generate graphs. Tests of significant differences were identified using a non-parametric test (specifically the Kruskal–Wallis test) to determine the significance of the differences in means among groups (photosynthetic types plus ploidy levels). Phylogenetic generalised least squares (PGLS) models were performed to test for correlations while considering evolutionary relationships. Values of Pagel's lambda from zero to one represented the strength of the phylogenetic signal. A summary function in R was then run for each model to determine the adjusted multiple correlation coefficients (r^2) and statistical significances of covariates between variables ($p < 0.05$).

3 | RESULTS

3.1 | Stomatal characteristics

The non-parametric Kruskal–Wallis test showed that C_4 diploid grasses had significant shorter ($p < 0.05$) GCLs than either non-C_4 diploid populations or C_4 hexaploid and dodecaploid populations (Figure 2a). The analysis of ancestral state reconstructions for GCL in all diploids also showed that the common ancestor of C_4 *A. semialata* had shorter GCLs than those of C_3–C_4 or C_3 plants (Figure 2a; Figure 3 node Q vs. nodes W and Z), indicating that cell shortening coincided with the origin of C_4 photosynthesis. However, there were no significant differences in GCW, GCV, GCSA to volume ratio (GCSA:GCV) and SD among diploids (Figure 2). GCL and GCW became larger as the ploidy levels increased in C_4 plants (Figures 2 and 3). Specifically, among C_4 grasses, there were significant positive associations ($p < 0.05$) between genome size and guard cell size (Figure 4a,b), which is consistent with previous studies (Beaulieu et al., 2008; Jordan et al., 2015; Lomax et al., 2009). However, for a given genome size, C_3 and C_3–C_4 plants had longer guard cells with a similar width to C_4 plants (Figures 2 and 3). GCL was therefore similar, but GCW was greater, in C_4 hexaploids compared with C_3 and C_3–C_4 diploids (Figure 2a,b). As a consequence, GCV was lowest in C_4 diploids, followed by C_3–C_4 and C_3 diploids, C_4 hexaploids, and C_4 dodecaploids (Figure 2c). However, C_3 and C_4 diploids had a significantly greater ($p < 0.05$) ratio of GCSA:GCV than hexaploids and dodecaploids (Figure 2d).

SCLs and widths in C_4 diploids were both significantly lower ($p < 0.05$) than in C_3–C_4 diploids, C_4 hexaploids and dodecaploids (Figure 2e,f). SD in C_4 and non-C_4 diploids was significantly higher ($p < 0.05$) than that in dodecaploids (Figure 2g). However, there were no significant differences in SD among the diploids with different photosynthetic types (Figure 2g). Calculated g_{max} based on stomatal size and density was significantly lower ($p < 0.05$) in C_4 populations than in C_3 and C_3–C_4 populations (Figure 2h). Compared to C_3 diploids, the g_{max} value was reduced by 40% in C_4 dodecaploids (Figure 2h). There was an offset in the log-log relationships between guard cell size and SD for C_4 plants in comparison with non-C_4 plants, particularly when guard cell size was measured via cell length (Figure 4c). However, the equivalent offset for the relationship with GCW was still able to distinguish C_3 from the combination of C_3–C_4 and C_4 types (Figure 4d).

3.2 | Dynamic responses of photosynthesis and stomatal conductance to light

C_3 and C_4 individuals showed different stomatal responses to a step change in the light environment, especially in dynamic responses of g_s (Figures 5 and S2–S4). For the dynamic responses of photosynthetic

13653040, 0, Downloaded from https://onlinelibrary.wiley.com/doi/10.1111/pce.15047 by University Of Sheffield, Wiley Online Library on [01/08/2024]. See the Terms and Conditions (https://onlinelibrary.wiley.com/terms-and-conditions) on Wiley Online Library for rules of use; OA articles are governed by the applicable Creative Commons License

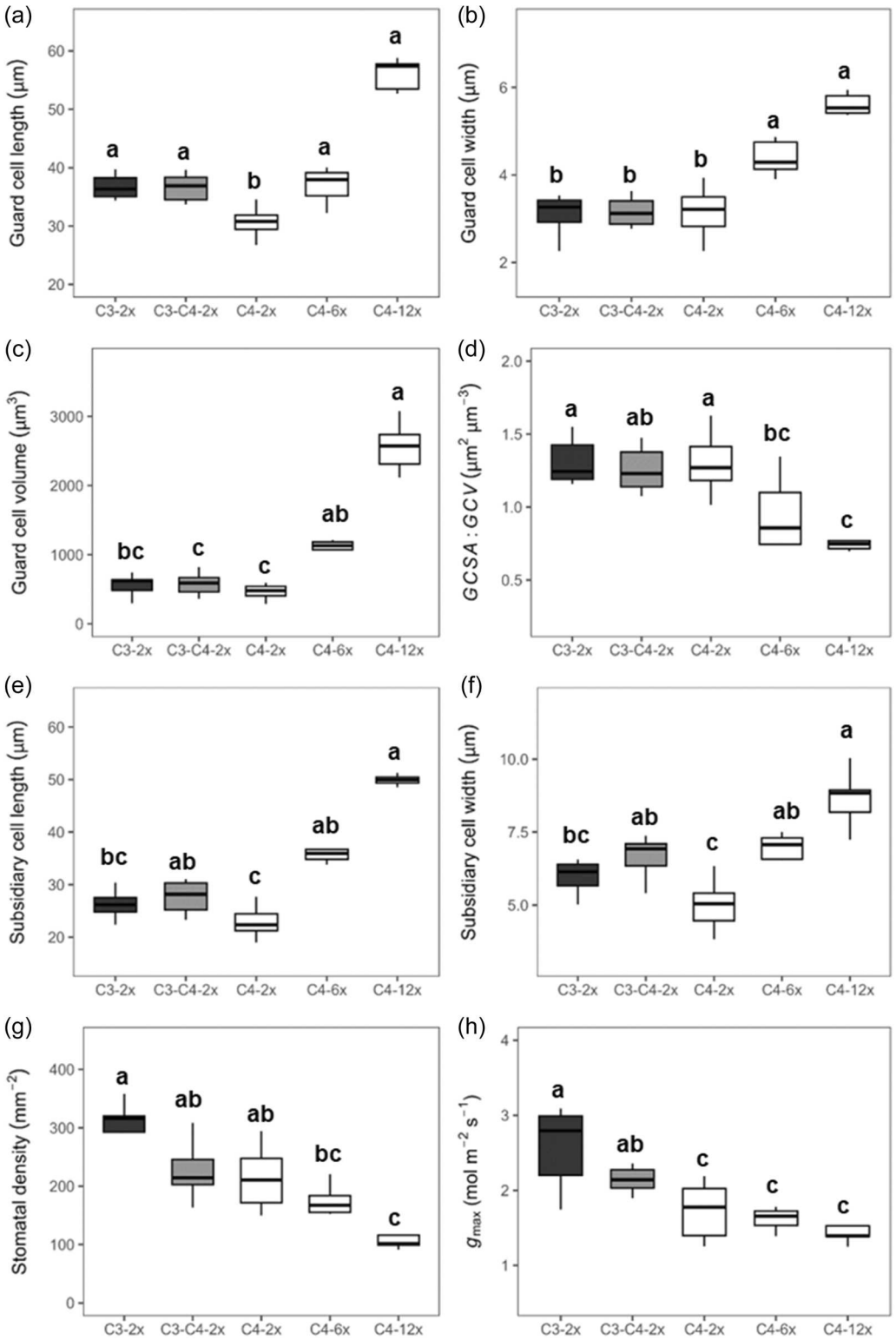

FIGURE 2 Guard cell length (a), guard cell width (b), guard cell volume (c), guard cell surface area to volume ratio (GCSA:GCV) (d), subsidiary cell length (e), subsidiary cell width (f), stomatal density (g), and maximum stomatal conductance (g_{max}) (h) in different groups of *Alloteropsis semialata*. C_3–2x included eight replicates, C_3–C_4–2x eleven replicates, C_4–2x seventeen replicates, C_4–6x seven replicates, and C_4–12x five replicates. Variables with significant group effects were subjected to a Kruskal-Wallis test, and groups that differed significantly were denoted with different letters ($p < 0.05$).

13653040, 0, Downloaded from https://onlinelibrary.wiley.com/doi/10.1111/pce.15047 by University Of Sheffield, Wiley Online Library on [01/08/2024]. See the Terms and Conditions (https://onlinelibrary.wiley.com/terms-and-conditions) on Wiley Online Library for rules of use; OA articles are governed by the applicable Creative Commons License

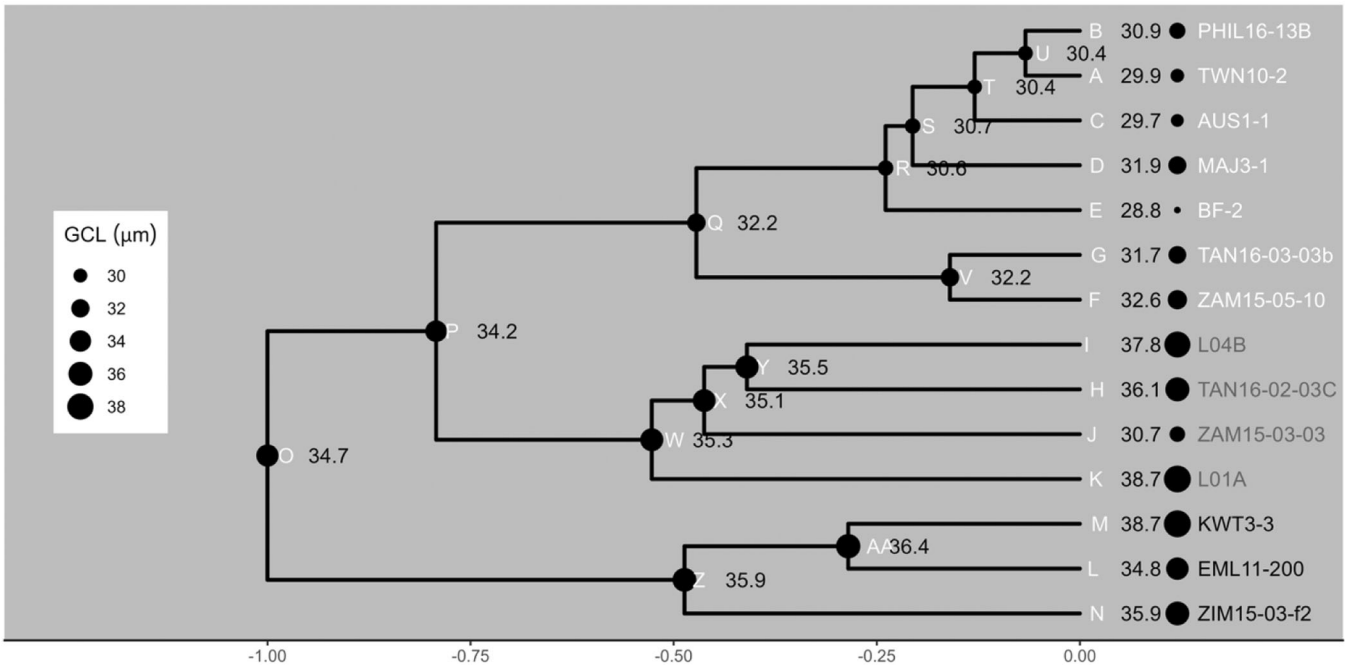

FIGURE 3 Ancestral state reconstruction of guard cell length (GCL) in *Alloteropsis semialata*. The measured and inferred values of GCL are mapped on a time-calibrated phylogeny of all diploids included in this study. Dot size and the colour ramp represent the absolute values of GCL, as observed for tips and inferred for ancestral nodes. Population names in different colours represent different photosynthetic types (C_3 in black, C_3–C_4 in grey, C_4 in white).

rate, the initial value of net CO_2 assimilation rate (A_0) at the initial PPFD of 100 μmol m^{-2} s^{-1} showed no significant variation, such that A_0 was lower than 5 μmol m^{-2} s^{-1} for all groups (Figure 5a). The rapid rise in net leaf CO_2 assimilation rate (A) in response to an increase in PPFD to 1000 μmol m^{-2} s^{-1} occurred within the first 10 min in all groups. However, it took double the time for A to reach a maximum steady state (A_s) in the C_4 dodecaploids than in the others. As expected, C_4 plants had higher A_s under high PPFD than C_3 and C_3–C_4 intermediates plants (Figure 5a).

The stomatal opening phase was characterised by an increase in g_s to a maximum steady-state value (G_s). The maximum rate of stomatal opening (SI_{max_i}) of C_3 plants was the steepest, followed by C_3–C_4 intermediate plants, C_4 diploid plants, C_4 hexaploid plants, and C_4 dodecaploid plants (Figure 5b; Table S3). In particular, the maximum slopes of C_4 hexaploids and dodecaploids were significantly ($p < 0.05$) lower than those of C_3 diploids (Table S3). The rates of stomatal opening also differed among C_4 plants with differing ploidy levels (Figure 5b; Table S3). As expected, C_4 diploids had a significant ($p < 0.05$) higher SI_{max_i} than C_4 dodecaploids (Table S3). Fitted model parameters (for details, see Figure S1) describing the stomatal opening response showed significant differences ($p < 0.05$) in non-C_4 plants compared to C_4 dodecaploid plants (Table S3). In particular, C_3 and C_3–C_4 diploids had significantly lower ($p < 0.05$) values of the opening time constant (k_i), representing faster stomatal opening than dodecaploids (Table S3). To isolate the effects of photosynthetic pathway evolution from those of polyploidy, which only occurs in the C_4 types, we made an ancestral state reconstruction of k_i for the diploids only. This showed that the common ancestor of C_4 *A. semialata* had a similar stomatal opening speed to that of C_3–C_4 plants (Figure 6 Node q vs. Node w; Table S3). In contrast, the common ancestor of C_4 and C_3–C_4 *A. semialata* had a slower stomatal opening speed than that of C_3 plants (Figure 6 Node p vs. Node z; Table S3).

On the other hand, stomatal closure in response to a decrease in PPFD from 1000 to 100 μmol m^{-2} s^{-1} followed a similar pattern in all groups (Figures 5 and S5), despite C_4 dodecaploids displaying the lowest value of final steady-state A and g_s (Figure 5). Compared to the speed of stomatal responses to increasing light conditions, the speed of stomatal closing was substantially faster. Nevertheless, its rapidity was still an order of magnitude slower than that of A. An almost immediate decrease of A to a new target of steady-state was established before g_s reaching the final steady-state value.

3.3 | Factors explaining variation in stomatal opening speed

In general, PGLS analysis showed relationships between cell size and parameters of stomatal opening responses in C_4 plants (Figure 7). There was a significant ($p < 0.05$) positive relationship between the opening time constant (k_i) and GCL, SCL or GCV across the C_4 plants (Figure 7). Larger guard cells, subsidiary cells, and higher GCV were characterised by higher values of k_i, corresponding to slower stomatal opening speed (Figure 7). For a given GCL, C_4 hexaploid plants had a slower stomatal opening speed than C_3 diploid plants (Figure 7a).

13653040, 0, Downloaded from https://onlinelibrary.wiley.com/doi/10.1111/pce.15047 by University Of Sheffield, Wiley Online Library on [01/08/2024]. See the Terms and Conditions (https://onlinelibrary.wiley.com/terms-and-conditions) on Wiley Online Library for rules of use; OA articles are governed by the applicable Creative Commons License

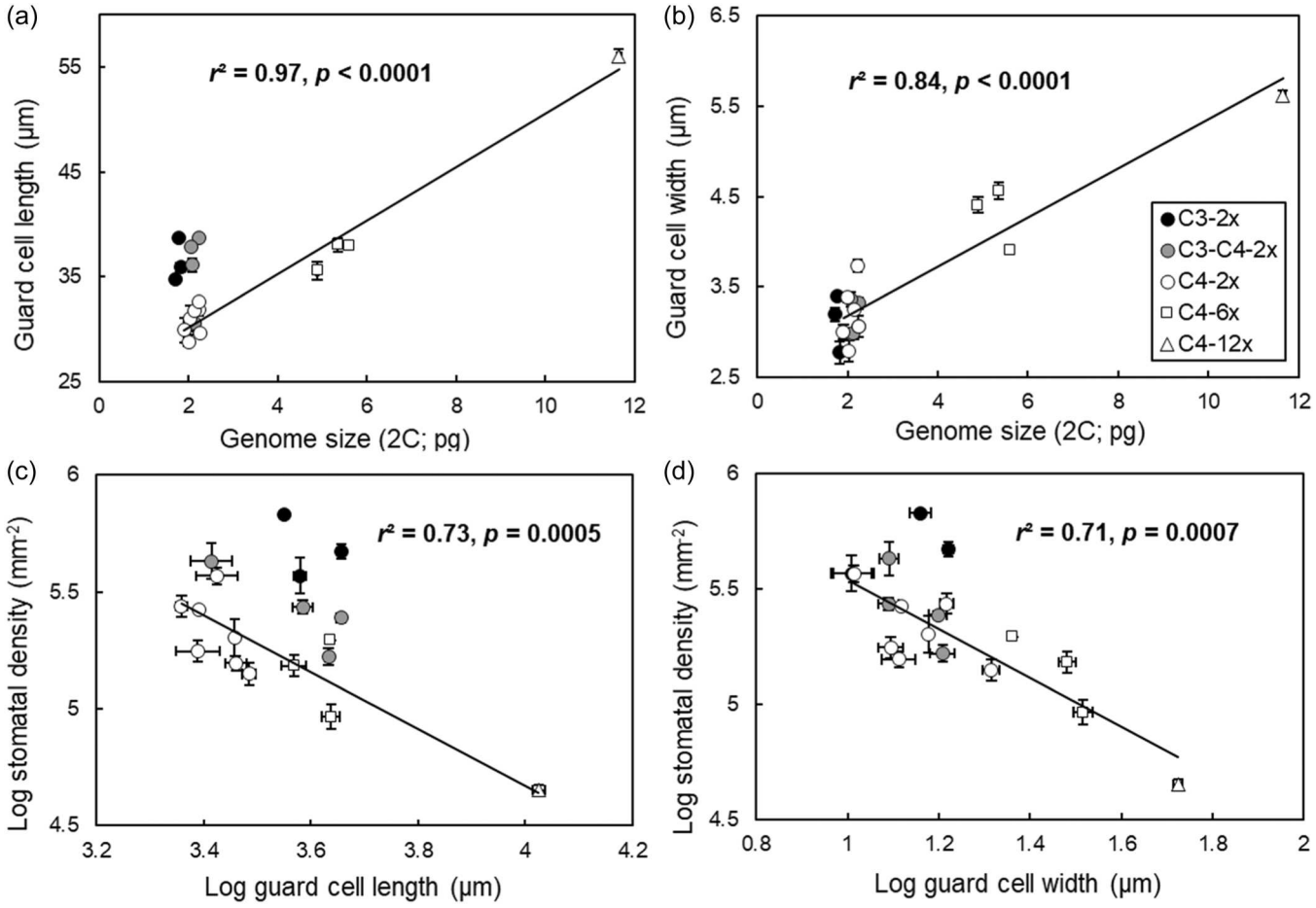

FIGURE 4 Relationship between genome size and guard cell length (a); the relationship between genome size and guard cell width (b); the log–log relationship between guard cell length and stomatal density (c); and the log–log relationship between guard cell width and stomatal density (d) in different groups of *Alloteropsis semialata* (C_3–2x black circles, C_3–C_4–2x grey circles, C_4–2x white circles, C_4–6x white squares and C_4–12x white triangles). Replication for each population is provided in Table S2. Points and error bars represent individual means and standard errors.

Besides the effects of guard cell size and photosynthetic pathway, local climates played an additional role in stomatal behaviour. Figures 6 and 8a showed significant variation ($p < 0.05$) among C_4 diploids in the values of k_i, which ranged fourfold from 1.7 to 6.8 min. To isolate the effects of environment from those of photosynthetic type and polyploidy, we therefore analysed the relationship of k_i in C_4 diploids to climate. Crucially, there was a significant ($p < 0.05$) negative relationship between k_i and annual precipitation among the seven populations of C_4 diploid plants (Figure 8a). This means that the speed of stomatal opening was faster in C_4 diploids that have migrated into wetter environments. The opening lag time (λ_i) for stomatal opening was also significantly ($p < 0.05$) influenced by annual precipitation (Figure 8b). However, unlike the rapidity of stomatal opening, C_4 diploids in the wetter environments had longer lag times in their responses to increasing light (Figure 8b).

Finally, regressions of the light-saturated photosynthetic rate (A_{sat}) versus opening time constant k_i for *A. semialata* in C_4 type showed that populations with higher values of A_{sat} had a faster stomatal opening speed (Figure 9). In addition, C_4 plants had slower opening stomata (higher k_i) than C_3 plants for a given photosynthetic rate (Figure 9).

4 | DISCUSSION

4.1 | Guard cells shortened following the evolution of C_4 photosynthesis in diploids

The common ancestor of C_4 *A. semialata* had shorter guard cells than C_3–C_4 or C_3 plants (Figures 2a and 3), implying that the initial evolution of C_4 photosynthesis led to a shortening of guard cells before diversification in this species. This finding, in conjunction with previous work showing that smaller guard cells for a given density is a general property of C_4 grass stomata (Taylor et al., 2012), suggests that the size of guard cells is adjusted after the evolution of C_4 photosynthesis, and indicates a close link between photosynthetic physiology and guard cell size. One of the potential explanations for

13653040, 0, Downloaded from https://onlinelibrary.wiley.com/doi/10.1111/pce.15047 by University Of Sheffield, Wiley Online Library on [01/08/2024]. See the Terms and Conditions (https://onlinelibrary.wiley.com/terms-and-conditions) on Wiley Online Library for rules of use; OA articles are governed by the applicable Creative Commons License

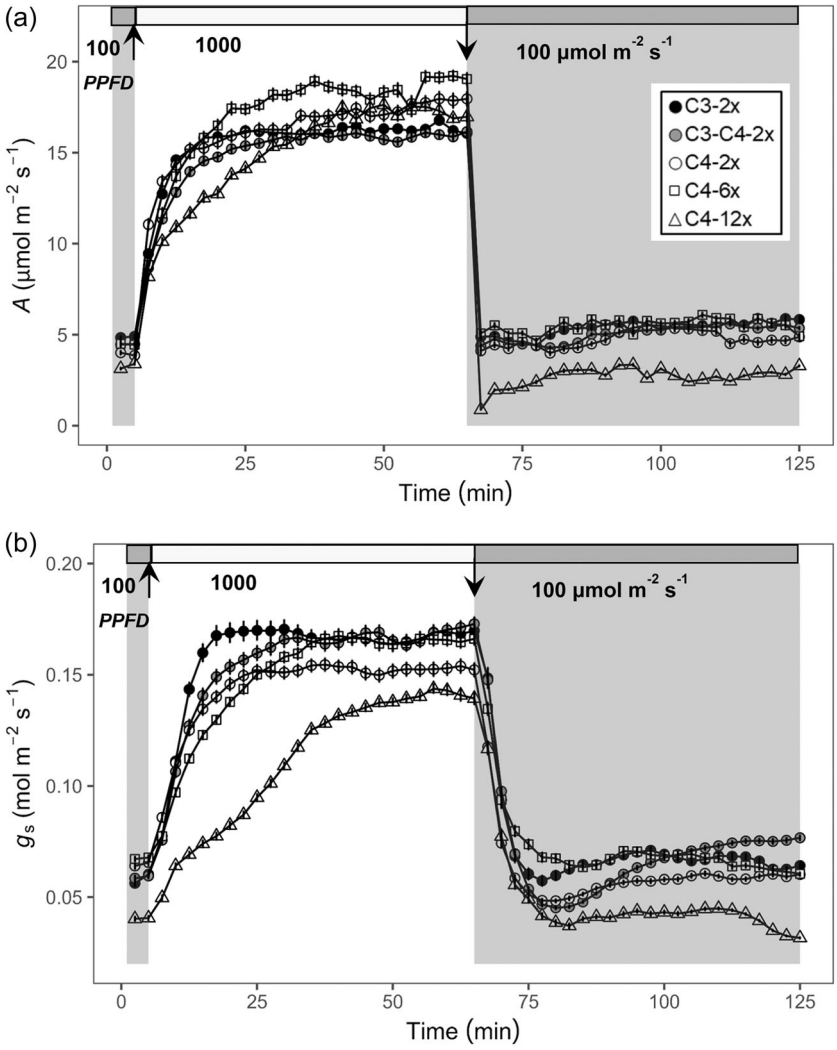

FIGURE 5 Dynamic responses of photosynthesis (a) and stomatal conductance (b) to step changes in light in different groups of *Alloteropsis semialata* (C_3–2x black circles, C_3–C_4–2x grey circles, C_4–2x white circles, C_4–6x white squares, and C_4–12x white triangles). Points and error bars represent individual means and standard errors at least five individuals. The shaded area represents PPFD decreased to 100 µmol m^{-2} s^{-1}.

this would be that the rapid light-induction of C_4 photosynthesis requires faster stomatal opening, which is facilitated by smaller guard cells.

There is no coincident change in GCW during C_4 evolution in *A. semialata* (Figures 2b and S6). Width changes after polyploid formation in C_4 *A. semialata* show that these are possible if all cell types across the leaf are enlarged. However, within a ploidy level, width may be limited in these grasses by the development of stomatal complexes within ordered rows of cells (i.e., cell files), such that their proximity to adjacent rows constrains their width (McKown & Bergmann, 2020). GCW may be further limited by association with subsidiary cells, whose shape and signalling responses are highly coordinated with those of guard cells (Gray et al., 2020; McKown & Bergmann, 2018). However, SCW did decrease after the evolution of C_4 photosynthesis (Figure 2f), showing that width changes are possible within stomatal complexes. This may be important, because subsidiary cells are thought to adjust the range of pore apertures and stomatal responsiveness (Raissig et al., 2017). In fact, subsidiary cells may be important regulators of the speeds of stomatal opening and closure in grasses (Chen et al., 2017; Raissig et al., 2017).

SD, on the other hand, shows considerable overlap among diploid populations of *A. semialata*. Even though the C_3 populations have significantly higher SD than C_4 hexaploid and dodecaploid populations (Figure 2g), two of the C_3 populations have values that overlap with the C_4 range (Figure 4c), showing that this trait is not directly associated with photosynthetic type in the same way as guard cell size (Figures S7–S9). More generally, variation among other species in stomatal size and density is inversely related, such that C_4 species tend to have lower stomatal densities than C_3 plants (McAusland et al., 2016; Taylor et al., 2012). Our data imply that this general difference in density arises as a secondary adaptation after the change in guard cell size.

Among the C_4 populations of *A. semialata* that differ in ploidy levels, larger guard cells have a slower stomatal response to increasing light, which is consistent with previous studies of cell size effects on stomatal dynamics (Drake et al., 2013; Franks & Beerling, 2009; Hetherington & Woodward, 2003; Lawson & Blatt, 2014). The size relationship arises from a lower surface-area-to-volume ratio in larger guard cells, which limits the capacity of ion pumping and solute transport across the plasma membrane to increase cellular concentrations of osmoticants (Lawson &

13653040, 0, Downloaded from https://onlinelibrary.wiley.com/doi/10.1111/pce.15047 by University Of Sheffield, Wiley Online Library on [01/08/2024]. See the Terms and Conditions (https://onlinelibrary.wiley.com/terms-and-conditions) on Wiley Online Library for rules of use; OA articles are governed by the applicable Creative Commons License

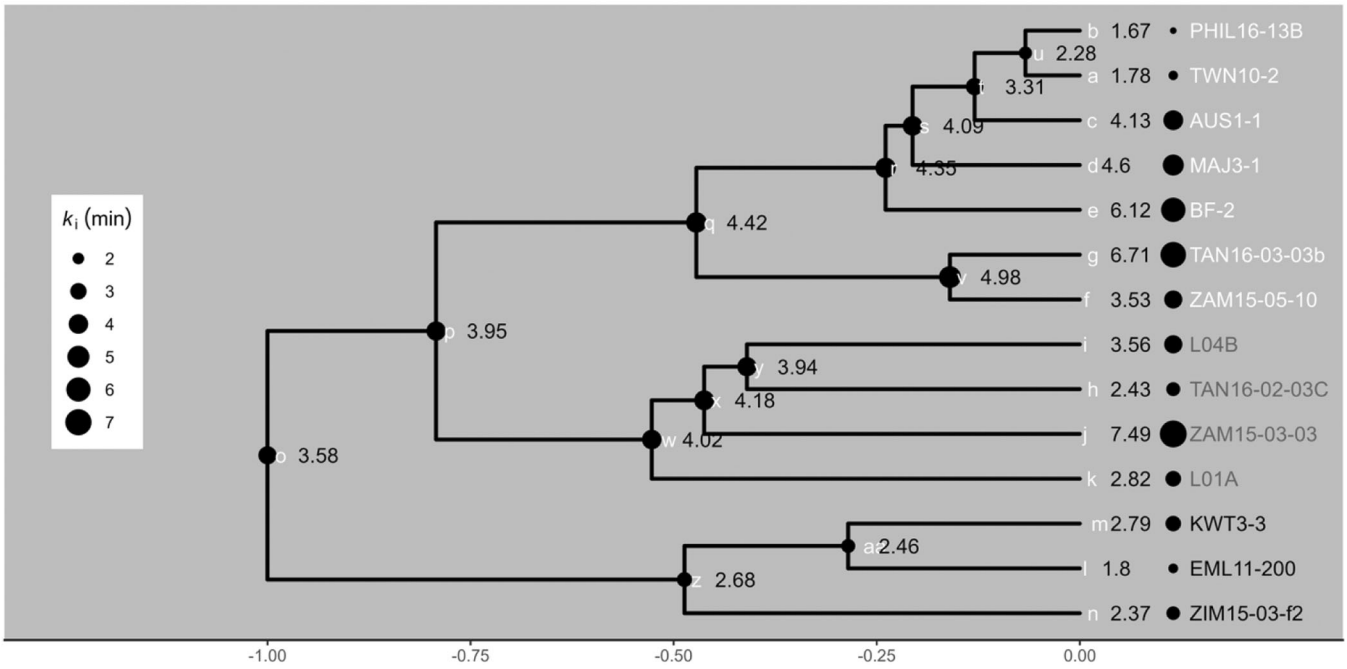

FIGURE 6 Ancestral state reconstruction of opening time constant (k_i) in *Alloteropsis semialata*. The measured and inferred values of k_i are mapped on a time-calibrated phylogeny of all diploids included in this study. Dot size and the colour ramp represent the absolute values of k_i, as observed for tips and inferred for ancestral nodes. Population names in different colours represent different photosynthetic types (C_3 in black, C_3–C_4 in grey, C_4 in white).

Blatt, 2014; Raven, 2014). Polyploid formation and its association with larger cells therefore leads directly to slower stomata. However, cell size is not the only determinant of stomatal opening and closing speeds, and other factors including guard cell shape, mechanical constraints and biochemical characteristics also play critical roles (Franks & Farquhar, 2007; McAusland et al., 2016; Ozeki et al., 2022; Raven, 2014).

If all else were equal, the evolution of shorter guard cells in C_4 diploid populations of *A. semialata* would therefore be expected to increase both opening and closing speeds in response to fluctuating light. However, our data indicate that this is not the case, implicating further changes in stomatal biology during the transition to C_4 photosynthesis.

4.2 | Transition to C_3–C_4 intermediate physiology initially slows stomatal opening

Our data show that some of the C_4 diploids have a similar stomatal opening speed to those of C_3 and C_3–C_4 plants, such that there is no overall difference in speed among diploids with different photosynthetic types (Figure 6; Table S3). However, there is considerable variation in opening speed among the diploid C_4 plants, despite limited variation in GCL or GCV (Figures 2a,d and 6). The evidence therefore shows a marked diversification of stomatal function in *A. semialata* following the evolution of C_4 photosynthesis. But did the first C_3–C_4 or C_4 plants in this species have stomata that opened at a slower or similar speed to those of their C_3 sisters?

Ancestral state reconstruction of the opening time constant among diploids shows that the common ancestor of C_4 and C_3–C_4 plants in our study had a slower opening speed than that of the C_3 plants (Figures 6 and S10). Subsequent diversification within the C_4 clade has been associated with mean annual rainfall (Figure 8). Ancestral state reconstruction shows that C_4 physiology emerged once in *A. semialata* in a relatively dry climate (Figure 8). In summary, this evidence therefore indicates that the initial divergence between populations using C_3 photosynthesis, from those in which carbon fixation occurred partially (C_3–C_4) or wholly (C_4) via PEPC, was associated with a change in the stomatal opening speed (Figure 6). Subsequent diversification among C_4 populations as they migrated across the paleo-tropics led to the repeated evolution of faster stomata in wetter climate regions (Figure 8a).

A potential mechanism underlying these changes in stomatal opening rate is implied by the relationship of k_i to A_{sat}. The best current models assume that stomatal opening speed is biochemically limited by the ATP supply from cyclic and noncyclic photosynthetic electron transport (Lawson & Blatt, 2014; Matthews et al., 2020; Ng & Jarvis, 1980; Raven, 2014). Bellasio et al. (2017) developed a dynamic hydro-mechanical and biochemical model which showed that a lag in ATP production may mechanistically account for both the lag phase of stomatal response to increasing light, and stomatal opening speed. A lowering of photosynthetic capacity and/or disruption of guard cell ATP supply during the emergence of C_3–C_4 and C_4 photosynthesis are therefore plausible explanations for our observation of slower stomatal opening. The observation that the

13653040, 0, Downloaded from https://onlinelibrary.wiley.com/doi/10.1111/pce.15047 by University Of Sheffield, Wiley Online Library on [01/08/2024]. See the Terms and Conditions (https://onlinelibrary.wiley.com/terms-and-conditions) on Wiley Online Library for rules of use; OA articles are governed by the applicable Creative Commons License

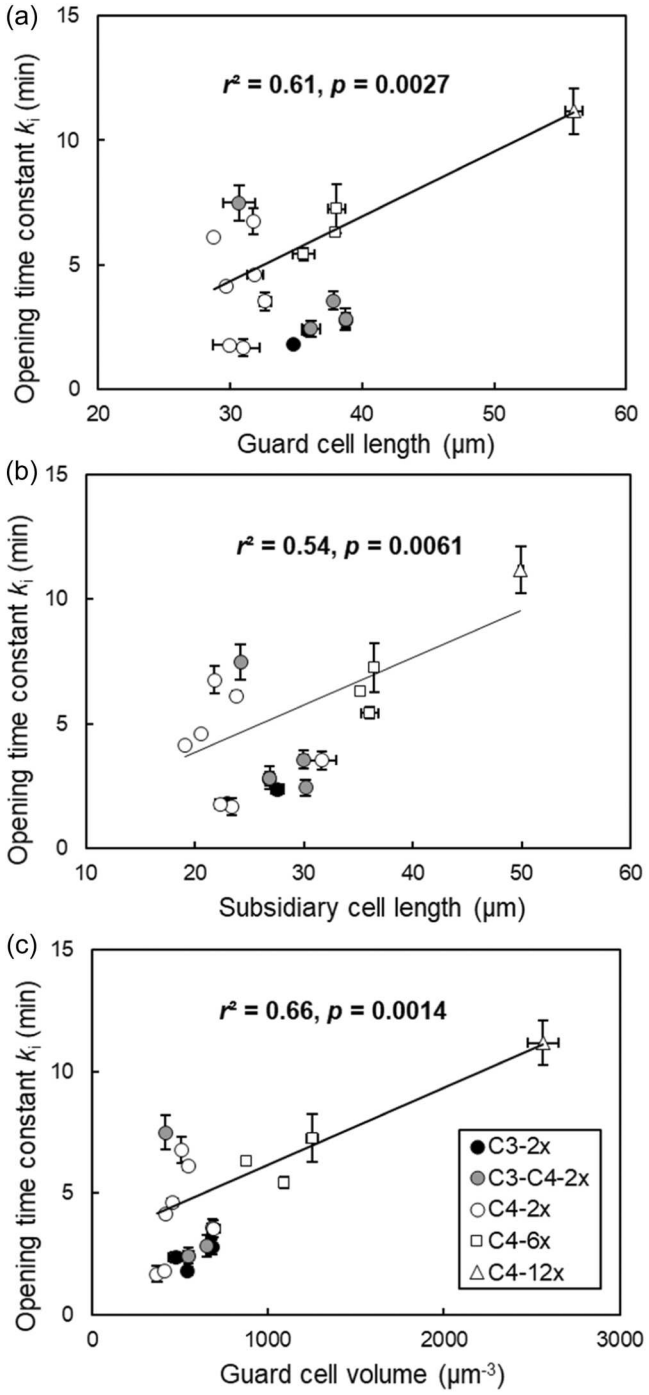

FIGURE 7 Relationship between guard cell length and opening time constant k_i (a); the relationship between subsidiary cell length and opening time constant k_i (b); and the relationship between guard cell volume and opening time constant k_i (c) in different groups of *Alloteropsis semialata* (C_3–2x black circles, C_3–C_4–2x grey circles, C_4–2x white circles, C_4–6x white squares, and C_4–12x white triangles). Replications of each population are provided in Table S2. Points and error bars represent individual means and standard errors.

initial, maximum rates of stomatal opening are similar in C_4 and non-C_4 plants (Figures 5, S5, and S11; Table S3) support this explanation, implying that opening is limited by the supply of energy or solutes, rather than the ion pumping capacity of guard cells. An alternative explanation could be that the blue or red light sensitivity of stomatal opening are disrupted by C_4 pathway evolution. However, new evidence suggests that these mechanisms are conserved across C_3 and C_4 types of *A. semialata* (Bernardo et al., 2023).

C_4 photosynthesis is unlikely to be very efficient when it first evolves. In *A. semialata*, the process arises through a small number of changes to anatomy and biochemistry (Dunning, Moreno-Villena, et al., 2019; Lundgren et al., 2019). Lateral gene transfer subsequently contributes to more rapid improvements in the catalytic efficiency of key C_4 enzymes, including PEPC (Phansopa et al., 2020). At the same time, leaf gas exchange is also likely optimised through the regulation of SD, and the formation and patterning of mesophyll airspace (Lundgren et al., 2019; Sugano et al., 2010). Our data imply that biochemical integration of stomatal function with C_4 photosynthetic metabolism may be an important aspect of that optimisation process.

4.3 | Adaptation to wetter climates accelerates stomatal opening speed in C_4 plants

Guard cell size and photosynthetic type are the dominant effects on stomatal opening speed in *A. semialata*. However, within the C_4 diploid type, the speed of stomatal responses to increasing light conditions differs significantly among populations (Figures 6 and 7), implying secondary adaptation of stomatal opening speed during diversification (Drake et al., 2013; Raven, 2014). This observation could be explained partly in the context of environmental characteristics across the geographical distribution of this species, with the stomatal opening time constant significantly related to annual precipitation in C_4 diploids (Figure 8a). This shows that when *A. semialata* C_4 plants have migrated into wetter habitats, their stomatal opening adapted by becoming faster. However, we also observed that the opening lag time was also significantly correlated with annual precipitation (Figure 8b), such that a longer lag time is coupled to a faster opening speed when C_4 diploids migrate into wetter environments.

Xiong et al. (2018) showed that a terrestrial herb (*Gossypium hirsutum*) had slower stomatal opening than a wet habitat species (*Centella asiatica*). Slow stomatal opening during shade-sun transitions may transiently limit CO_2 assimilation, if water is sufficient. The observed change in opening speed may serve as an adaptation to overcome this limitation in environmental contexts where water conservation is not critical. Conversely, the water-conserving effects of stomata that are not fully open may be more important for plant performance in drier habitats than transient CO_2-limitation.

5 | CONCLUSIONS

Our analysis suggests that the origin of C_4 photosynthesis led to a reduction in GCL, but this shortening of guard cells in C_4 plants occurred after a slowing of stomatal opening associated with the initial establishment of C_3–C_4 intermediate and then C_4 metabolism. This result is inconsistent with the hypothesis that smaller guard cells

13653040, 0, Downloaded from https://onlinelibrary.wiley.com/doi/10.1111/pce.15047 by University Of Sheffield, Wiley Online Library on [01/08/2024]. See the Terms and Conditions (https://onlinelibrary.wiley.com/terms-and-conditions) on Wiley Online Library for rules of use; OA articles are governed by the applicable Creative Commons License

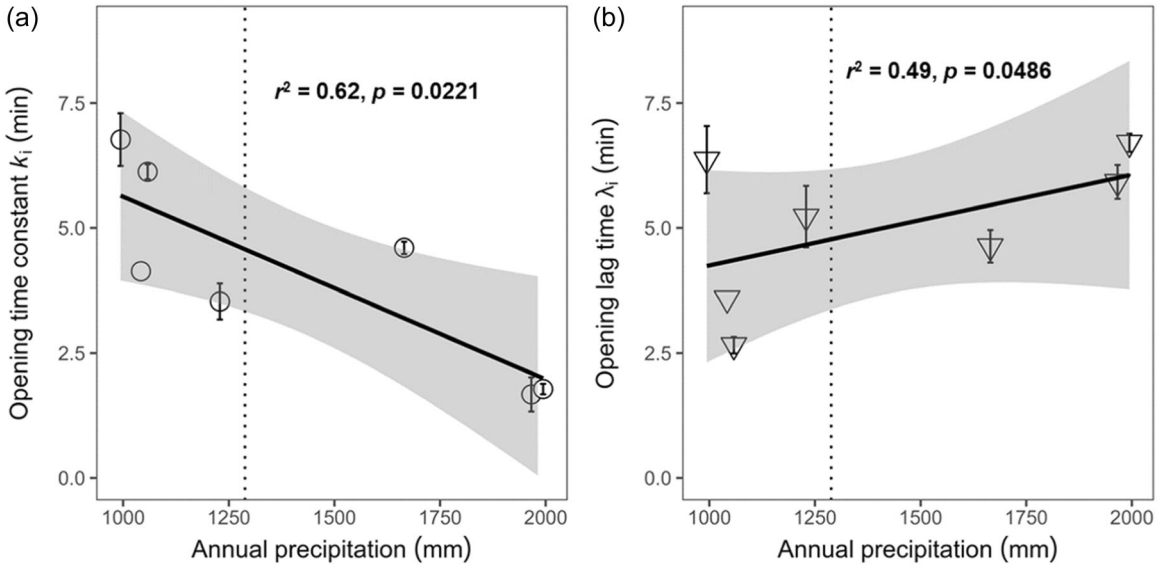

FIGURE 8 Relationship between annual precipitation and opening time constant k_i in C_4 diploids (a); the relationship between annual precipitation and opening lag time λ_i in C_4 diploids (b). Replications of each population are provided in Table S2. Points and error bars represent individual means and standard errors. The dotted vertical line indicates the inferred position of the ancestor of C_4 *Alloteropsis semialata* included in this study.

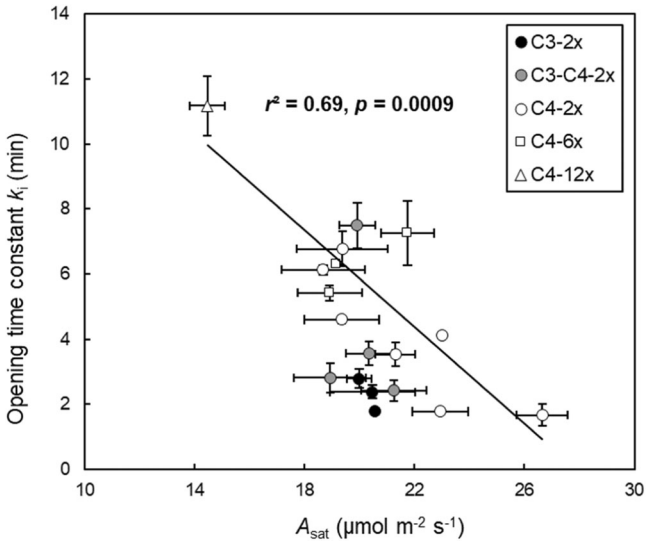

FIGURE 9 Relationship between the light-saturated photosynthetic rate (A_{sat}) and opening time constant k_i in different groups of *Alloteropsis semialata* (C_3–2x black circles, C_3–C_4–2x grey circles, C_4–2x white circles, C_4–6x white squares, and C_4–12x white triangles). Replications of each population are provided in Table S2. Points and error bars represent individual means and standard errors.

arising from C_4 pathway evolution have faster responses to light than in C_3 plants, and shows that the picture is more nuanced than implied by previous work in crops. The association of stomatal opening speed with the rate of photosynthesis implies a disruption to guard cell energy supply during the establishment of C_4 physiology. Stomatal opening was further slowed after polyploid formation, presumably by the enlargement of guard cells and the associated reduction in GCV. However, stomatal opening was accelerated in diploids by adaptation to wet climate conditions and the optimisation of C_4 photosynthesis during the diversification of this species. Our work provides explanations for the diversity of stomatal function across the range of a single species, demonstrating the importance of an interplay between physiological innovation, cell structure and function in the evolutionary dynamics of stomatal behaviour.

ACKNOWLEDGEMENTS

We thank the China Scholarship Council (CSC) for financial support to Yanmin Zhou. We also thank Pascal-Antoine Christin for providing plant materials and a phylogenetic tree of *A. semialata* species, Matheus Bianconi for R code to extract the parameters of climate, Sahr Mian for genome size measurements, and Julie Gray and Pascal-Antoine Christin for their constructive comments on the manuscript.

DATA AVAILABILITY STATEMENT

The data that supports the findings of this study are available in Zenodo at https://zenodo.org/records/12743587

ORCID

Yanmin Zhou http://orcid.org/0000-0002-1837-9261
Colin P. Osborne http://orcid.org/0000-0002-7423-3718

REFERENCES

Abadi, S., Azouri, D., Pupko, T. & Mayrose, I. (2019) Model selection may not be a mandatory step for phylogeny reconstruction. *Nature Communications*, 10, 934.

Alenazi, A.S., Bianconi, M.E., Middlemiss, E., Milenkovic, V., Curran, E.V., Sotelo, G. et al. (2023) Leaf anatomy explains the strength of C_4 activity within the grass species *Alloteropsis semialata*. *Plant, Cell & Environment*, 46, 2310–2322.

13653040, 0, Downloaded from https://onlinelibrary.wiley.com/doi/10.1111/pce.15047 by University Of Sheffield, Wiley Online Library on [01/08/2024]. See the Terms and Conditions (https://onlinelibrary.wiley.com/terms-and-conditions) on Wiley Online Library for rules of use; OA articles are governed by the applicable Creative Commons License

Beaulieu, J.M., Leitch, I.J., Patel, S., Pendharkar, A. & Knight, C.A. (2008) Genome size is a strong predictor of cell size and stomatal density in angiosperms. *New Phytologist*, 179(4), 975–986.

Bellasio, C., Quirk, J., Buckley, T.N. & Beerling, D.J. (2017) A dynamic hydro-mechanical and biochemical model of stomatal conductance for C_4 photosynthesis. *Plant Physiology*, 175(1), 104–119.

Bernardo, E.L., Sales, C.R.G., Cubas, L.A., Vath, R.L. & Kromdijk, J. (2023) A comparison of stomatal conductance responses to blue and red light between C_3 and C_4 photosynthetic species in three phylogenetically-controlled experiments. *Frontiers in Plant Science*, 14, 1253976.

Bianconi, M.E., Dunning, L.T., Curran, E.V., Hidalgo, O., Powell, R.F., Mian, S. et al. (2020) Contrasted histories of organelle and nuclear genomes underlying physiological diversification in a grass species. *Proceedings of the Royal Society B*, 287(1938), 20201960.

Bouckaert, R., Vaughan, T.G., Barido-Sottani, J., Duchêne, S., Fourment, M., Gavryushkina, A. et al. (2019) BEAST 2.5: an advanced software platform for Bayesian evolutionary analysis. *PLoS Computational Biology*, 15(4), e1006650.

Bouckaert, R.R. (2010) DensiTree: making sense of sets of phylogenetic trees. *Bioinformatics*, 26(10), 1372–1373.

Bräutigam, A. & Gowik, U. (2016) Photorespiration connects C_3 and C_4 photosynthesis. *Journal of Experimental Botany*, 67(10), 2953–2962.

Brestic, M., Zivcak, M., Hauptvogel, P., Misheva, S., Kocheva, K., Yang, X. et al. (2018) Wheat plant selection for high yields entailed improvement of leaf anatomical and biochemical traits including tolerance to non-optimal temperature conditions. *Photosynthesis Research*, 136(2), 245–255.

Chen, Z.-H., Chen, G., Dai, F., Wang, Y., Hills, A., Ruan, Y.-L. et al. (2017) Molecular evolution of grass stomata. *Trends in Plant Science*, 22(2), 124–139.

Doležel, J., Greilhuber, J. & Suda, J. (2007) Estimation of nuclear DNA content in plants using flow cytometry. *Nature Protocols*, 2(9), 2233–2244.

Drake, P.L., Froend, R.H. & Franks, P.J. (2013) Smaller, faster stomata: scaling of stomatal size, rate of response, and stomatal conductance. *Journal of Experimental Botany*, 64(2), 495–505.

Dunn, J., Hunt, L., Afsharinafar, M., Meselmani, M.A., Mitchell, A., Howells, R. et al. (2019) Reduced stomatal density in bread wheat leads to increased water-use efficiency. *Journal of Experimental Botany*, 70(18), 4737–4748.

Dunning, L.T., Moreno-Villena, J.J., Lundgren, M.R., Dionora, J., Salazar, P., Adams, C. et al. (2019) Key changes in gene expression identified for different stages of C_4 evolution in *Alloteropsis semialata*. *Journal of Experimental Botany*, 70(12), 3255–3268.

Dunning, L.T., Olofsson, J.K., Parisod, C., Choudhury, R.R., Moreno-Villena, J.J., Yang, Y. et al. (2019) Lateral transfers of large DNA fragments spread functional genes among grasses. *Proceedings of the National Academy of Sciences of the United States of America*, 116(10), 4416–4425.

Durand, M., Brendel, O., Buré, C. & Le Thiec, D. (2020) Changes in irradiance and vapour pressure deficit under drought induce distinct stomatal dynamics between glasshouse and field-grown poplars. *New Phytologist*, 227(2), 392–406.

Faralli, M., Cockram, J., Ober, E., Wall, S., Galle, A., Van Rie, J. et al. (2019) Genotypic, developmental and environmental effects on the rapidity of g_s in wheat: impacts on carbon gain and water-use efficiency. *Frontiers in Plant Science*, 10, 492.

Fick, S.E. & Hijmans, R.J. (2017) WorldClim 2: new 1-km spatial resolution climate surfaces for global land areas. *International journal of climatology*, 37(12), 4302–4315.

Franks, P.J. & Beerling, D.J. (2009) Maximum leaf conductance driven by CO_2 effects on stomatal size and density over geologic time. *Proceedings of the National Academy of Sciences*, 106(25), 10343–10347.

Franks, P.J. & Farquhar, G.D. (2001) The effect of exogenous abscisic acid on stomatal development, stomatal mechanics, and leaf gas exchange in *Tradescantia virginiana*. *Plant Physiology*, 125(2), 935–942.

Franks, P.J. & Farquhar, G.D. (2007) The mechanical diversity of stomata and its significance in gas-exchange control. *Plant Physiology*, 143(1), 78–87.

Gray, A., Liu, L. & Facette, M. (2020) Flanking support: how subsidiary cells contribute to stomatal form and function. *Frontiers in Plant Science*, 11, 881.

Hetherington, A.M. & Woodward, F.I. (2003) The role of stomata in sensing and driving environmental change. *Nature*, 424(6951), 901–908.

Hijmans, R.J. (2023). Geographic Data Analysis and Modeling [R package raster version 3.6-20].

Jordan, G.J., Carpenter, R.J., Koutoulis, A., Price, A. & Brodribb, T.J. (2015) Environmental adaptation in stomatal size independent of the effects of genome size. *New Phytologist*, 205(2), 608–617.

Kaiser, E., Correa Galvis, V. & Armbruster, U. (2019) Efficient photosynthesis in dynamic light environments: a chloroplast's perspective. *Biochemical Journal*, 476(19), 2725–2741.

Lawson, T. & Blatt, M.R. (2014) Stomatal size, speed, and responsiveness impact on photosynthesis and water use efficiency. *Plant Physiology*, 164(4), 1556–1570.

Linder, H.P., Lehmann, C.E.R., Archibald, S., Osborne, C.P. & Richardson, D.M. (2018) Global grass (Poaceae) success underpinned by traits facilitating colonization, persistence and habitat transformation. *Biological Reviews*, 93(2), 1125–1144.

Lomax, B.H., Woodward, F.I., Leitch, I.J., Knight, C.A. & Lake, J.A. (2009) Genome size as a predictor of guard cell length in *Arabidopsis thaliana* is independent of environmental conditions. *New Phytologist*, 181(2), 311–314.

Long, S.P., ZHU, X.G., Naidu, S.L. & Ort, D.R. (2006) Can improvement in photosynthesis increase crop yields? *Plant, cell & environment*, 29(3), 315–330.

Lundgren, M.R., Christin, P.A., Escobar, E.G., Ripley, B.S., Besnard, G., Long, C.M. et al. (2016) Evolutionary implications of C_3–C_4 intermediates in the grass *Alloteropsis semialata*. *Plant, cell & environment*, 39(9), 1874–1885.

Lundgren, M.R., Mathers, A., Baillie, A.L., Dunn, J., Wilson, M.J., Hunt, L. et al. (2019) Mesophyll porosity is modulated by the presence of functional stomata. *Nature Communications*, 10(1), 2825.

Matthews, J.S.A., Vialet-Chabrand, S. & Lawson, T. (2020) Role of blue and red light in stomatal dynamic behaviour. *Journal of Experimental Botany*, 71(7), 2253–2269.

Matthews, J.S.A., Vialet-Chabrand, S.R.M. & Lawson, T. (2017) Diurnal variation in gas exchange: the balance between carbon fixation and water loss. *Plant Physiology*, 174(2), 614–623.

McAusland, L., Vialet-Chabrand, S., Davey, P., Baker, N.R., Brendel, O. & Lawson, T. (2016) Effects of kinetics of light-induced stomatal responses on photosynthesis and water-use efficiency. *New Phytologist*, 211(4), 1209–1220.

McKown, K.H. & Bergmann, D.C. (2018) Grass stomata. *Current Biology*, 28(15), R814–R816.

McKown, K.H. & Bergmann, D.C. (2020) Stomatal development in the grasses: lessons from models and crops (and crop models). *New Phytologist*, 227(6), 1636–1648.

Ng, P. & Jarvis, P. (1980) Hysteresis in the response of stomatal conductance in *Pinus sylvestris* L needles to light: observations and a hypothesis. *Plant, Cell & Environment*, 3(3), 207–216.

Olofsson, J.K., Bianconi, M., Besnard, G., Dunning, L.T., Lundgren, M.R., Holota, H. et al. (2016) Genome biogeography reveals the intraspecific spread of adaptive mutations for a complex trait. *Molecular Ecology*, 25(24), 6107–6123.

13653040, 0, Downloaded from https://onlinelibrary.wiley.com/doi/10.1111/pce.15047 by University Of Sheffield, Wiley Online Library on [01/08/2024]. See the Terms and Conditions (https://onlinelibrary.wiley.com/terms-and-conditions) on Wiley Online Library for rules of use; OA articles are governed by the applicable Creative Commons License

Olofsson, J.K., Curran, E.V., Nyirenda, F., Bianconi, M.E., Dunning, L.T., Milenkovic, V. et al. (2021) Low dispersal and ploidy differences in a grass maintain photosynthetic diversity despite gene flow and habitat overlap. *Molecular Ecology*, 30(9), 2116–2130.

Olofsson, J.K., Dunning, L.T., Lundgren, M.R., Barton, H.J., Thompson, J., Cuff, N. et al. (2019) Population-specific selection on standing variation generated by lateral gene transfers in a grass. *Current Biology*, 29(22), 3921–3927.e5.

Orr, D.J., Pereira, A.M., da Fonseca Pereira, P., Pereira-Lima, Í.A., Zsögön, A. & Araújo, W.L. (2017) Engineering photosynthesis: progress and perspectives. *F1000Research*, 6, 1891.

Ozeki, K., Miyazawa, Y. & Sugiura, D. (2022) Rapid stomatal closure contributes to higher water use efficiency in major C_4 compared to C_3 Poaceae crops. *Plant Physiology*, 189(1), 188–203.

Phansopa, C., Dunning, L.T., Reid, J.D. & Christin, P.-A. (2020) Lateral gene transfer acts as an evolutionary shortcut to efficient C_4 biochemistry. *Molecular Biology and Evolution*, 37(11), 3094–3104.

Raimondeau, P., Bianconi, M.E., Pereira, L., Parisod, C., Christin, P.A. & Dunning, L.T. (2023) Lateral gene transfer generates accessory genes that accumulate at different rates within a grass lineage. *New Phytologist*, 240(5), 2072–2084.

Raissig, M.T., Matos, J.L., Anleu Gil, M.X., Kornfeld, A., Bettadapur, A., Abrash, E. et al. (2017) Mobile MUTE specifies subsidiary cells to build physiologically improved grass stomata. *Science*, 355(6330), 1215–1218.

Raven, J.A. (2014) Speedy small stomata? *Journal of Experimental Botany*, 65(6), 1415–1424.

Sugano, S.S., Shimada, T., Imai, Y., Okawa, K., Tamai, A., Mori, M. et al. (2010) Stomagen positively regulates stomatal density in *Arabidopsis*. *Nature*, 463(7278), 241–244.

Taylor, S.H., Franks, P.J., Hulme, S.P., Spriggs, E., Christin, P.A., Edwards, E.J. et al. (2012) Photosynthetic pathway and ecological adaptation explain stomatal trait diversity amongst grasses. *New Phytologist*, 193(2), 387–396.

Vialet-Chabrand, S., Dreyer, E. & Brendel, O. (2013) Performance of a new dynamic model for predicting diurnal time courses of stomatal conductance at the leaf level. *Plant, cell & environment*, 36(8), 1529–1546.

Vialet-Chabrand, S.R.M., Matthews, J.S.A., McAusland, L., Blatt, M.R., Griffiths, H. & Lawson, T. (2017) Temporal dynamics of stomatal behavior: modeling and implications for photosynthesis and water use. *Plant Physiology*, 174(2), 603–613.

Weyers, J.D. & Meidner, H. (1990). Methods in stomatal research.

Weyers, J.D.B. & Johansen, L.G. (1985) Accurate estimation of stomatal aperture from silicone rubber impressions. *New Phytologist*, 101(1), 109–115.

Xiong, D., Douthe, C. & Flexas, J. (2018) Differential coordination of stomatal conductance, mesophyll conductance, and leaf hydraulic conductance in response to changing light across species. *Plant, cell & environment*, 41(2), 436–450.

SUPPORTING INFORMATION

Additional supporting information can be found online in the Supporting Information section at the end of this article.

How to cite this article: Zhou, Y. & Osborne, C.P. (2024) Stomatal dynamics in *Alloteropsis semialata* arise from the evolving interplay between photosynthetic physiology, stomatal size and biochemistry. *Plant, Cell & Environment*, 1–13. https://doi.org/10.1111/pce.15047

13653040, 0, Downloaded from https://onlinelibrary.wiley.com/doi/10.1111/pce.15047 by University Of Sheffield, Wiley Online Library on [01/08/2024]. See the Terms and Conditions (https://onlinelibrary.wiley.com/terms-and-conditions) on Wiley Online Library for rules of use; OA articles are governed by the applicable Creative Commons License